Lawrence Berkeley Laboratory

UNIVERSITY OF CALIFORNIA

Materials & Molecular Research Division

Submitted to the Journal of Nuclear Materials

DISSOLUTION OF ZrO_2 BY LIQUID ZIRCALOY

D.R. Olander

January 1983

Prepared for the U.S. Department of Energy under Contract DE-AC03-76SF00098

DISCLAIMER

DISSOLUTION OF ZrO_2 BY LIQUID ZIRCALOY

by D.R. Olander

Materials and Molecular Research Division of the Lawrence Berkeley Laboratory and the Department of Nuclear Engineering, University of California, Berkeley, CA 94720

This work was supported by the Director, Office of Energy Research, Office of Basic Energy Sciences, Materials Sciences Division of the U.S. Department of Energy under contract #DE-AC03-76SF00098.

I INTRODUCTION

Detailed analyses of fuel element behavior during a degraded core accident in a nuclear reactor are being developed in numerous laboratories. An important aspect of this modeling is the prediction of the consequences of temperatures in excess of the melting point of the Zircaloy cladding of the fuel rod, which is ∿ 1850°C. Prior to melting, reaction of solid Zircaloy with steam forms a scale of ZrO_2 on the exterior of the cladding. Upon melting of the remaining metallic portion of the cladding, Hagen's experiments show that the liquid can be held in place by its still-solid skin(1). Consequently, the course of a reactor accident which results in an uncovered and overheated core is dependent upon the thickness and integrity of the oxide scale on the cladding exterior surface. The thickness of the oxide layer depends strongly upon the time spent in the temperature range 1200 - 1850°C(2). The mechanism and conditions for rupture of the oxide skin, however, are not well established.

The Severe Core Damage Analysis Package (SCDAP) which is under development at the Idaho National Engineering Laboratory (3) uses a stress criterion for oxide layer breach; when the fracture stress of ZrO_2 is exceeded because of expansion which accompanies melting of the metal, the oxide layer splits and the molten metal flows out of the breach. Chung and Gehl(4), on the other hand, have proposed a chemical mechanism by which the oxide skin can fail. When melting takes place, the oxygen solubility and diffusivity in the metal increases abruptly, thereby greatly enhancing the ability of the metal to dissolve the oxide. At the same time, the oxide layer is replenished by continued absorption of oxygen from reaction with the external steam. This process is not affected by melting of the metal inside of the oxide skin. If oxide dissolution proceeds more rapidly than corrosion, the oxide layer will disappear and the liquid metal will flow from the unprotected area. Ultimately, the Zircaloy-steam reaction converts all metal to ZrO_2, but before this process is completed, considerable relocation of cladding and fuel can occur as a result of the mobility of the liquid metal.

The present work is an attempt to model quantitatively the process of chemical thinning of an oxide skin in contact with a layer of molten Zircaloy. In performing the calculation, two features are neglected. First, the corrosion rate at the steam-oxide interface is known to be strongly influenced by the fraction of hydrogen in the steam(5). We neglect this "steam starvation" effect and assume that the Zircaloy corrosion proceeds as in oxidation of the solid metal under conditons of unlimited steam. Second, molten Zircaloy is known to be a good solvent for the UO_2 fuel (6). The chemical interaction between molten Zircaloy and UO_2 is neglected in the present study. Enough is known about the "steam starvation" and "fuel liquefaction" processes to acknowledge their importance in analysis of fuel behavior in reactor accidents. However, they cannot at this time be quantitatively modeled. Oxide skin dissolution, on the other hand, can be described with reasonable rigor using conventional scaling theory. Consequently, we present such an analysis with the realization that it will eventually need to be augmented to incorporate the two other phenomena discussed above. These simplifications lead to the following specific conditions on the analysis:

1. Stoichiometric ZrO_2 is maintained at the steam-oxide interface at all times.
2. No oxygen or metal transfer occurs across the interface between the molten metal and the fuel.

II ANALYSIS

The initial state of the system consists of a slab of solid Zircaloy of thickness L_{20} with an average oxygen content C_{20}. Upon melting, the oxygen in the metal is assumed to become homogenized in the liquid so that the concentration is uniform at $t = 0$. The thickness of the inital oxide layer is denoted by L_{10} and its composition is assumed to be that of stoichiometric zirconia, which has an oxygen concentration denoted by C_o. This inital state is shown in the upper diagram of Fig. 1. The lower sketch of this figure shows the system after interaction of the liquid metal and the oxide scale. The thickness of the oxide(1) and the liquid metal(2) are L_1 and L_2, respectively. Oxygen concentration distributions are sketched as heavy lines. The boundary concentrations C_o, C_a and C_b are obtained from the zirconium-oxygen phase diagram at the specified system temperature. These are shown on Fig. 2 for a temperature of 2000°C. The two zones of the corrosion couple are marked on the isotherm in Fig. 2.

The segment between the concentrations C_a and C_b on the isotherm of Fig. 2 represents the oxide-liquid metal interface in the diffusion couple. As indicated in Fig. 1, this interface moves with a speed v relative to the steam-oxide boundary, which is taken as a fixed reference plane for the entire system. This velocity may be positive or negative depending on the relative rates of oxide dissolution by the liquid metal and growth by reaction with steam. The outer boundary of the liquid metal moves with velocity v_{Zr}. Motion of this surface occurs in response to the volume change which takes place when the metal is converted to oxide. This volume effect is characterized by the Pilling-Bedworth ratio B, which is the ratio of the zirconium atom density in the liquid metal to that in the oxide. Volume changes of the metal due to oxygen dissolution are neglected. The boundary velocities are given by:

$$v = dL_1/dt \qquad (1)$$

$$v_{Zr} = dL_1/dt + dL_2/dt = v + dL_2/dt$$

Conservation of zirconium is expressed by:

$$L_{10}/B + L_{20} = L_1/B + L_2 \tag{2}$$

Taking the derivative of this equation with respect to time and combining with Eq(1) yields:

$$v_{Zr} = \left(\frac{B - 1}{B}\right) v \tag{3}$$

so that only the velocity v is an independent variable. The object of the analysis is to compute the time dependence of v, or, alternatively, the thickness of the oxide layer as a function of time.

Diffusion Equations

The oxygen diffusion equations in zones 1 and 2 must be solved subject to appropriate boundary conditions and a flux-matching condition at the oxide-metal interface. In expressing conservation of oxygen in each zone, a coordinate reference plane must be specified. These planes need not be identical to the fixed plane at the steam-oxide boundary. Gross motion of zirconium in each zone with respect to the coordinate reference plane for that zone must be taken into account in formulating the oxygen balance. Oxygen diffusion relative to the zirconium atoms of a zone is assumed to be expressed by Fick's law. Transport of oxygen by movement of the zirconium lattice with respect to the coordinate reference plane appears in the oxygen mass balance as a convective term.

In zone 1, the coordinate reference plane is chosen as the steam-oxide boundary, with the coordinate x indicated in Fig. 1. In this coordinate system, the zirconium lattice exhibits no gross motion, so the oxygen diffusion equation has no convective term:

$$\frac{\partial C_1}{\partial t} = D_1 \frac{\partial^2 C_1}{\partial x^2} \tag{4}$$

where C_1 is the oxygen concentration in the oxide at position x and time t and D_1 is the diffusivity of oxygen in zirconia. The initial condition is:

$$C_1(x,0) = C_o \tag{5}$$

The boundary condition at the steam-oxide boundary is:

$$C_1(0,t) = C_o \tag{6}$$

which reflects the first condition stated at the end of Section I. At the oxide-metal interface, the oxygen concentration in the oxide phase is:

$$C_1\ (L_1,t) = C_a \tag{7}$$

In zone 2, the coordinate reference plane is chosen as the moving oxide-metal interface, with distance from this plane denoted by y. In this coordinate system, the gross velocity of the zirconium is the difference between the velocity v_{Zr} arising from volume changes due to conversion of metal to oxide and the motion of the oxide-metal boundary, which imparts a negative velocity component. The convective velocity is thus $v_{Zr} - v = v/B$, where Eq(3) has been used to eliminate v_{Zr}. The oxygen diffusion equation in zone 2 is:

$$\frac{\partial C_2}{\partial t} - \frac{v}{B}\frac{\partial C_2}{\partial y} = D_2\frac{\partial^2 C_2}{\partial y^2} \qquad (8)$$

where C_2 and D_2 are the oxygen concentration and diffusivity, respectively, in the liquid metal. The initial and boundary conditions for Eq(8) are:

$$C_2(y,0) = C_{20} \qquad (9)$$

$$C_2(0,t) = C_b \qquad (10)$$

$$(\partial C_2/\partial y)_{L_2} = 0 \qquad (11)$$

The last of these conditions reflects the neglect of interaction between the liquid metal and the adjacent fuel, as discussed in Section I. Note that the infinite-medium approximation (i.e., $C_2(\infty,t) = C_{20}$) has not been used. Because of this, the corrosion process does not follow parabolic kinetics.

The final condition is an oxygen balance at the moving oxide-metal interface. In addition to Fick's law terms representing molecular diffusion fluxes, movement of the interface with respect to the zirconium atoms on either side of the interface generates convective fluxes of oxygen as well.

The equality of oxygen flows on either side of this interface is expressed by:

$$D_1\left(\frac{\partial C_1}{\partial x}\right)_{x=L_1} + vC_a = D_2\left(\frac{\partial C_2}{\partial y}\right)_{y=0} + \frac{v}{B}C_b \qquad (12)$$

Approximate Solution:

Because of the finite domain of the diffusion problem, exact solution of Eqs(4) - (12) is not possible. However, following Pawel(7) and Tucker et al(8), we seek solutions for C_1 and C_2 which satisfy the appropriate initial, boundary, and flux-matching conditions but not the diffusion equations. These approximate solutions are constrained to revert to the exact solutions for the infinite medium case.

The approximate solution in zone 1 is:

$$\frac{C_1 - C_a}{C_o - C_a} = \frac{\operatorname{erfc}\left(\frac{L_{10} - L_1}{2\sqrt{D_1 t}}\right) - \operatorname{erfc}\left(\frac{L_{10} - x}{2\sqrt{D_1 t}}\right)}{\operatorname{erfc}\left(\frac{L_{10} - L_1}{2\sqrt{D_1 t}}\right) - \operatorname{erfc}\left(\frac{L_{10}}{2\sqrt{D_1 t}}\right)} \qquad (13)$$

which satisfies Eqs(5) - (7) but not Eq(4). However, as $L_2 \to \infty$ and $L_{10} \to 0$, parabolic kinetics applies and Eq(13) reduces to the formula deduced by Pawel(9) for this case.

Zone 2 is a finite slab with one boundary moving with respect to the other. Pawel(7) and Tucker et. al. (8) approximate the solution in this zone by an infinite series of complementary error functions with the arguments:

$$\left(\frac{2nL_2 - y}{2\sqrt{D_2 t}}\right) \quad \text{and} \quad \left(\frac{2nL_2 + y}{2\sqrt{D_2 t}}\right)$$

where n = 0, 1, 2, ... However, the diffusion equation in the problem they treated did not contain a convective term as in Eq(8). In this case, to obtain an approximate solution which reduces to the exact result when $L_2 \to \infty$ and $L_{10} \to 0$, we use a complementary error function series with the arguments:

$$\frac{2nL_2 + (L_1 - L_{10})/B \pm y}{2\sqrt{D_2 t}}$$

The approximate solution for zone 2 can then be written as:

$$\frac{C_2 - C_{20}}{C_b - C_{20}} = \frac{F(y)}{F(0)} \tag{14}$$

where:

$$F = \operatorname{erfc}\left(\frac{b+y}{a}\right) + \operatorname{erfc}\left(\frac{2L_2+b-y}{a}\right) - \operatorname{erfc}\left(\frac{2L_2+b+y}{a}\right) - \operatorname{erfc}\left(\frac{4L_2+b-y}{a}\right)$$
$$+ \operatorname{erfc}\left(\frac{4L_2+b+y}{a}\right) + \operatorname{erfc}\left(\frac{6L_2+b-y}{a}\right) - \operatorname{erfc}\left(\frac{6L_2+b+y}{a}\right) - \operatorname{erfc}\left(\frac{8L_2+b-y}{a}\right) \tag{15}$$

In this equation, $a = 2(D_2 t)^{\frac{1}{2}}$ and $b = (L_1 - L_{10})/B$. The infinite series is cut off at $n = 4$. Eqs(14) and (15) satisfy Eqs(9) - (11) but not Eq(8). However, in a semi-infinite medium with no initial scale, the exact solution is recovered.

Substituting C_1 from Eq(13) and C_2 from Eqs (14) and (15) into Eq(12) and replacing v by dL_1/dt yields:

$$\frac{(C_o - C_a)\exp\left[-\frac{(L_{10}-L_1)^2}{4D_1 t}\right]}{\operatorname{erfc}\left(\frac{L_{10}-L_1}{2\sqrt{D_1 t}}\right) - \operatorname{erfc}\left(\frac{L_{10}}{2\sqrt{D_1 t}}\right)} - \frac{\sqrt{\pi t}\,(C_a - C_b/B)}{\sqrt{D_1}}\,\frac{dL_1}{dt}$$

$$= \sqrt{\frac{D_2}{D_1}}\,(C_b - C_{20})\,G \tag{16}$$

where:

$$G = \left\{\exp\left[-\left(\frac{b}{a}\right)^2\right] - 2\exp\left[-\left(\frac{2L_2+b}{a}\right)^2\right] + 2\exp\left[-\left(\frac{4L_2+b}{a}\right)^2\right] - 2\exp\left[-\left(\frac{6L_2+b}{a}\right)^2\right] + \exp\left[-\left(\frac{8L_2+b}{a}\right)^2\right]\right\} \div \left[\operatorname{erfc}\left(\frac{b}{a}\right) - \operatorname{erfc}\left(\frac{8L_2+b}{a}\right)\right] \tag{17}$$

The growth (or disappearance) of the oxide scale is obtained by integrating Eq(16) numerically with the initial condition $L_1(0) = L_{10}$. The metal zone thickness L_2 is given by Eq(2).

III RESULTS

In addition to the temperature, which determines the equilibrium oxygen concentrations at the phase boundaries (Fig. 2) and the diffusion coefficient of oxygen in the oxide (Ref. 9), the parameters which must be specified are:

L_{20}/L_{10} = initial ratio of metal to oxide

C_{20}/C_b = initial fractional oxygen saturation of the metal

D_1/D_2 = ratio of oxygen diffusivities in the oxide and the liquid metal

The first two of these parameters depends upon the time-temperature history of the specimen prior to melting, which determines the extent of oxidation of the solid metal. The diffusion coefficient of oxygen in liquid Zircaloy is unknown, but is probably larger than that in ZrO_2.

Figure 3 shows the results of the calculation at 2000°C for a specimen with an initial metal-to-oxide thickness ratio of 10. Two extreme values of the initial oxygen concentration in the metal are used, namely oxygen-free and 98% saturated. The diffusivity of oxygen in liquid Zr is taken to be four times larger than in the solid oxide.

For the initially oxygen-free metal (solid curves in Fig. 3), extensive "chemical thinning" of the oxide scale occurs; a 10-fold reduction in the oxide scale occurs at a dimensionless time of approximately unity. However, at larger times, the oxide skin starts to thicken and the entire specimen is converted to ZrO_2 at a dimensionless time of $\sim$ 1000. The diffusion coefficient of oxygen in zirconia at 2000°C is $\sim 6 \times 10^{-5}$ cm^2/s (9). If the specimen was initially 11 mm thick with a 1 mm thick oxide scale separating the metal from the steam environment, liquefacation of the metal causes the oxide sale to be reduced to a thickness of 10 μm after 1.7 s of contact with the liquid metal. The reason that the scale is not completely dissolved by the liquid is that the production of new oxide by transport of oxygen produced by decomposition of steam at the surface is inversely proportional to the scale thickness. At the time of the minimum scale thickness, the corrosion rate just balances the dissolution rate.

The dashed curves in Fig. 3 are the calculated results for the same initial metal-to-oxide thicknesses but with the metal 98% saturated with oxygen at t = 0. In this case, no thinning of the oxide scale occurs. Intermediate degrees of initial fractional saturation of the metal would produce results falling between the dashed and solid curves of Fig. 3. However, for the conditions chosen for the calculation, the entire specimen is converted to oxide in ∿ ½ h, irrespective of the initial oxygen content of the metal.

Calculations for initally oxygen-free metal in which the parameter D_1/D_2 was varied showed that both the dimensionless time D_1t/L_{10}^2 and the fractional oxide scale thickness L_1/L_{10} at the minimum of the latter are proportional to the diffusivity ratio. Thus, if the diffusion coefficient of oxygen in the liquid metal is only twice as large as that in the oxide instead of a factor of four greater as assumed in Fig. 3, the oxide layer is reduced to 20% of its initial thickness instead of 10% and twice as long is required to accomplish the thinning. These results are consistent with the expected effect of reduced oxygen mobility in the liquid metal. For all values of the ratio D_1/D_2 tested, the qualitative features of the curves shown in Fig. 3 remain unchanged. In particular, the oxide skin cannot be completely penetrated by dissolution in the liquid metal as long as unlimited steam oxidation continues to supply oxygen from the gaseous environment. However, extensive thinning may permit rupture of the scale by mechanical stresses.

Acknowledgement

This work was supported by the Director, Office of Energy Research, Office of Basic Energy Sciences, Materials Sciences Division of the U.S. Department of Energy under contract # DE-AC03-76SF00098.

References

1. S. Hagen and H. Malauscheck, Trans. Amer. Nucl. Soc. 33, 505 (1979).
2. S. Hagen, "Out of Pile Experiments on the High Temperature Behavior of Zry-4 Clad Fuel Rods", 6th Inter. Conf. on Zirconium in the Nuclear Industry, Vancouver, June (1982).
3. T.M. Howe and R.W. Miller, Trans. Amer. Nucl. Soc. 41, 456 (1982)
4. H.M Chung and S.M. Gehl, "Thermochemical Aspects of Fuel Road Material Interactions at 1900°C", Inter. Mtg. on Thermal Nuclear Reactor Safety Chicago, September (1982).
5. H.M. Chung and G.R. Thomas, "High Temperature Oxidation of Zircaloy in Hydrogen-Steam Mixtures", 6th Inter. Conf. on Zirconium in the Nuclear Industry, Vancouver, July (1982).
6. P. Hofmann, D. Kerwin-Peck and P. Nikolopoulous, "Phiscal and Chemical Phenomena Associated with the Dissolution of Solid UO_2 by Molen Zircaloy-4", 6th Inter. Conf. on Zirconium in the Nuclear Industry, Vancouver, July (1982).
7. R.E. Pawel, J. Nucl. Mater. 49, 281 (1973/1974).
8. M.O. Tucker et. al., J. Nucl. Mater. 74, 41 (1978).
9. R.E. Pawel, J. Electrochem. Soc. 126, 1111 (1979).

Figure Captions

1. Zr-O equilibrium phase diagram.

   Reference: Urbanic, V.R., "Oxidation of Zirconium Alloys in Steam at 1000 to 1850°C," Zirconium in the Nuclear Industry ASTM STP 633, A.L. Lowe, Jr. and G.W. Parry, Eds., American Society for Testing and Materials, 1977, pp. 168-181

2. Diagram for calculation the evolution of an oxide layer contacting a liquid metal.

3. Oxide layer and metal thickness changes as a function of time following liquefaction of the metal at 2000°C.

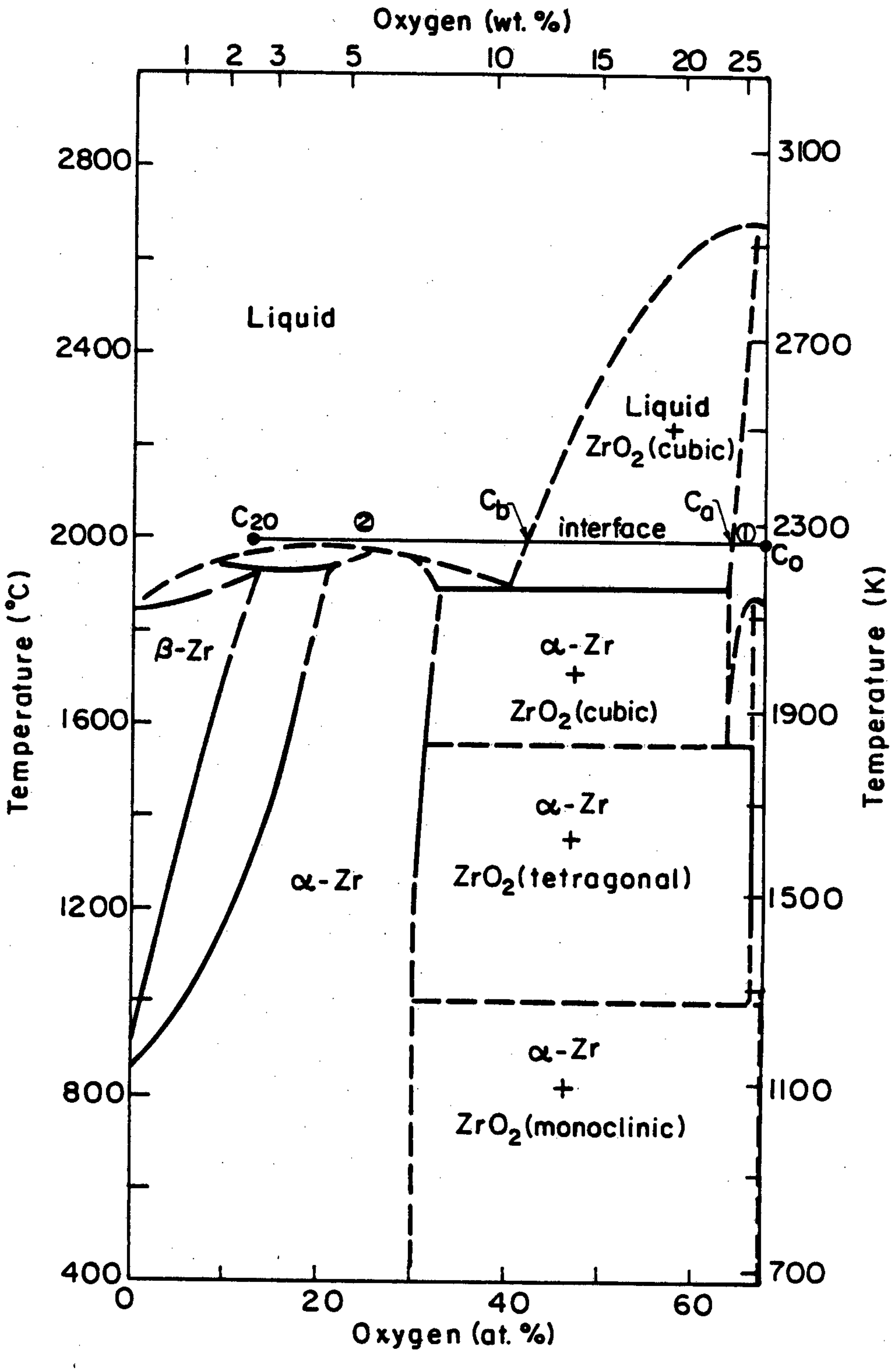

Oxygen (wt. %)
1 2 3 5 10 15 20 25
2800
2400
2000
1600
1200
800
400
3100
2700
2300
1900
1500
1100
700
Temperature (°C)
Temperature (K)
Liquid
Liquid + ZrO2 (cubic)
C20
2
Cb
interface
Ca
1
Co
β-Zr
α-Zr + ZrO2 (cubic)
α-Zr
α-Zr + ZrO2 (tetragonal)
α-Zr + ZrO2 (monoclinic)
0 20 40 60
Oxygen (at. %)
XBL 831-5071

Fig. 1

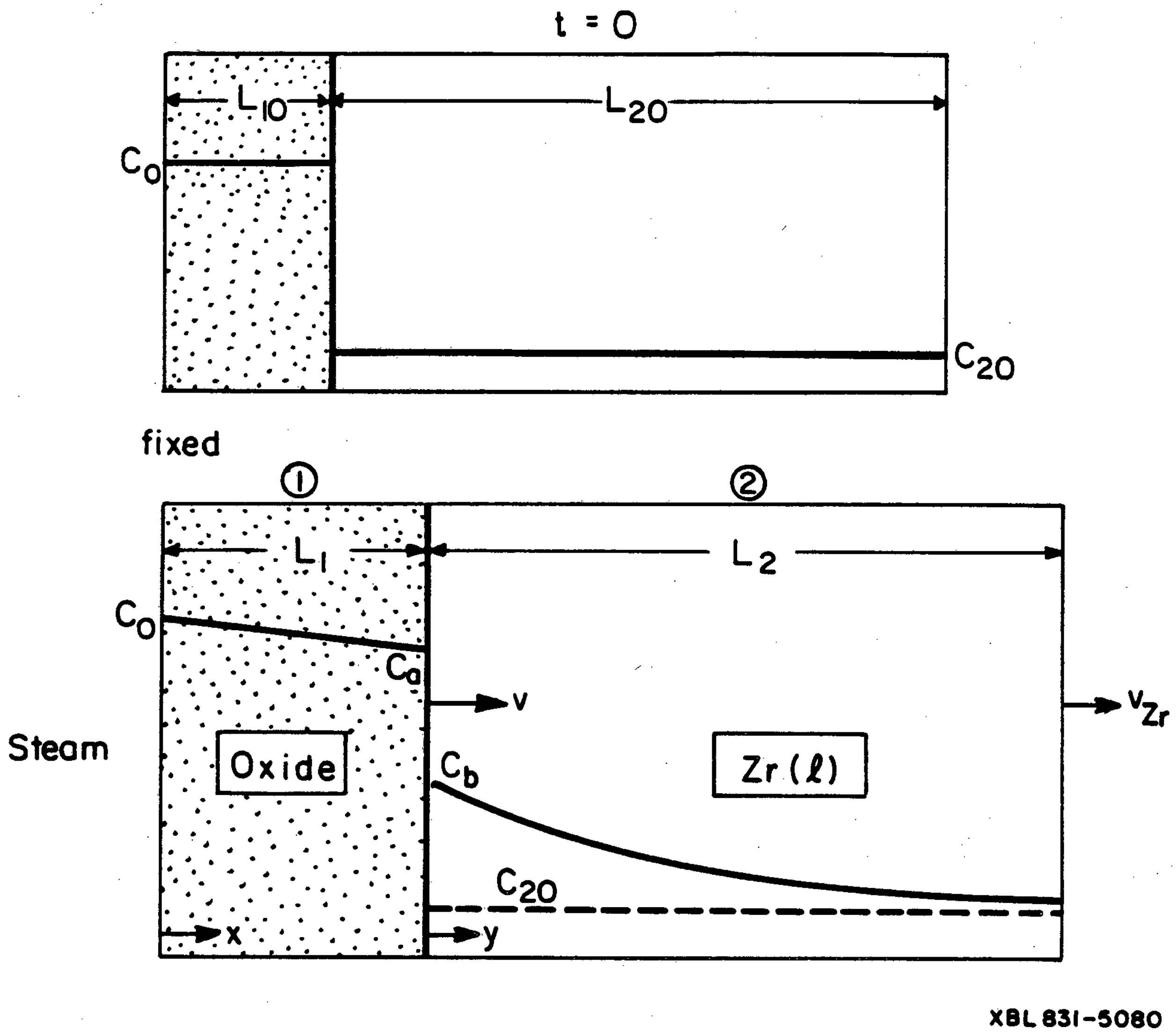
t = 0
L_{10}
L_{20}
C_0
C_{20}
fixed
①
②
L_1
L_2
C_0
C_a
v
v_{Zr}
Steam
Oxide
C_b
Zr (ℓ)
C_{20}
x
y
XBL 831-5080

Fig. 2

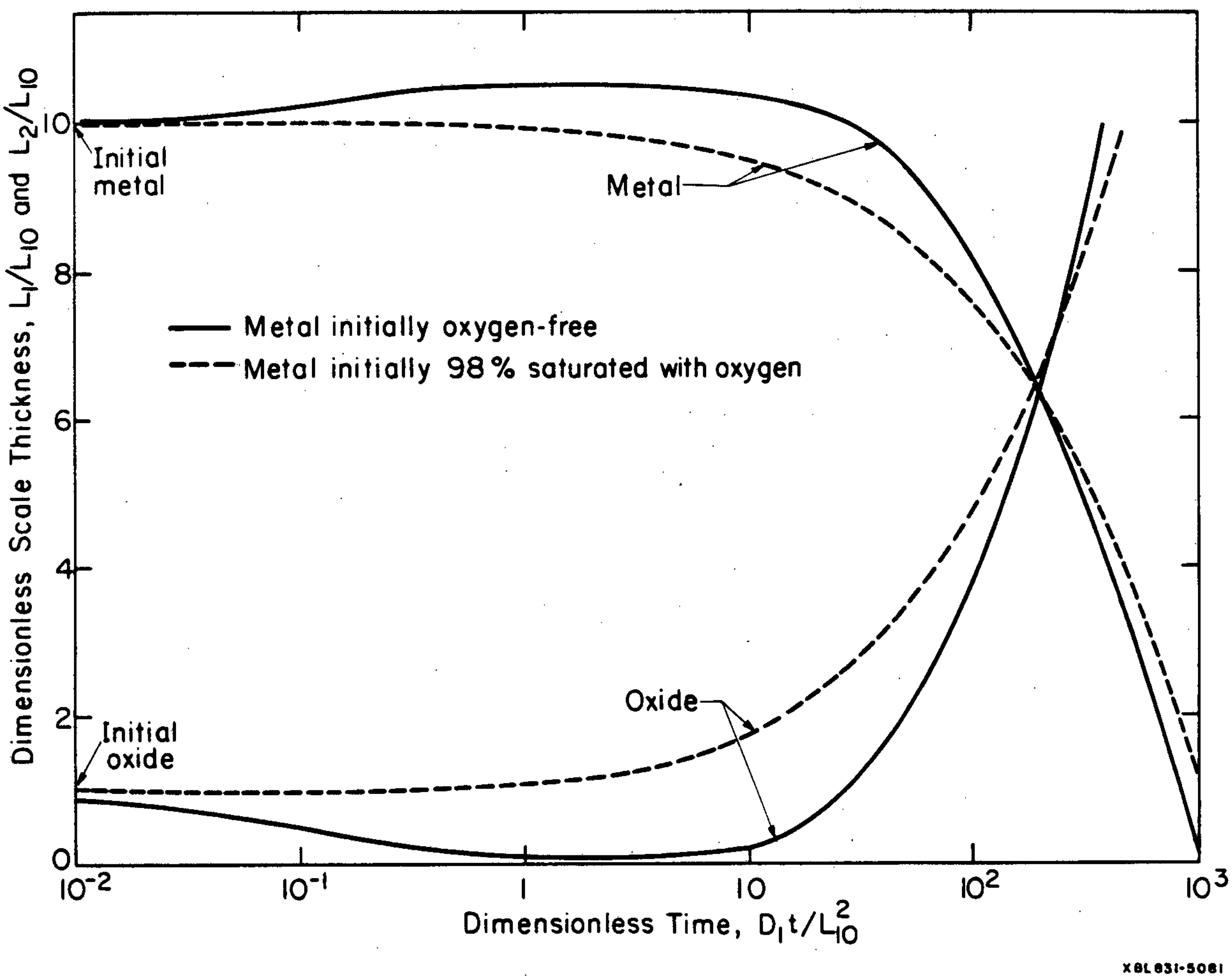

Dimensionless Scale Thickness, L_1/L_{10} and L_2/L_{10}
Dimensionless Time, D_1t/L_{10}^2
Initial metal
Metal
Metal initially oxygen-free
Metal initially 98% saturated with oxygen
Oxide
Initial oxide
0
2
4
6
8
10
10^{-2}
10^{-1}
1
10
10^2
10^3
XBL 831-5081

Fig. 3

TECHNICAL INFORMATION DEPARTMENT
LAWRENCE BERKELEY LABORATORY
UNIVERSITY OF CALIFORNIA
BERKELEY, CALIFORNIA 94720